

Oxidation of CO in H₂–CO mixtures catalyzed by platinum: alkali effects on rates and selectivity

Cristina Pedrero, Toshio Waku¹, Enrique Iglesia*

Department of Chemical Engineering, University of California at Berkeley, Berkeley, CA 94720, USA

Received 23 December 2004; revised 23 March 2005; accepted 6 April 2005

Available online 3 June 2005

Abstract

Turnover rates and selectivities for CO oxidation in H₂–CO–O₂ reactant mixtures are much greater on Pt clusters supported on Cs-modified SiO₂ than on clusters of similar size dispersed on SiO₂ or Al₂O₃ supports. Selectivity effects reflect the inhibition of spillover-mediated H₂ oxidation pathways on support surfaces. Infrared spectra showed that Cs, Rb, or Na titrates support hydroxyl groups required for these unselective pathways. These H₂ oxidation pathways are unaffected by competitive CO co-adsorption and can lead to significant selectivity losses during preferential CO oxidation in H₂-rich streams. CO oxidation selectivities on Pt are above 90%, even at H₂/CO ratios of ~100; much lower selectivities reported previously reflect contributions from spillover-mediated H₂ oxidation pathways on supports, which are not inhibited by CO co-reactants. Cs and Rb also increased turnover rates for monofunctional oxidation of CO on Pt cluster surfaces, apparently by disrupting the growth of chemisorbed CO monolayers, which prevent activation of O₂ co-reactants. The addition of 1.6 Cs/nm² to SiO₂ led to CO oxidation turnover rates more than 10 times higher than those on Pt/SiO₂ catalysts with similar Pt dispersion. CO monolayer growth processes are evident from a gradual decrease in CO oxidation rates during the initial stages of H₂–CO–O₂ reactions, which occurs simultaneously with an increase in intensity for chemisorbed CO infrared bands measured during reaction. This densification of chemisorbed CO monolayers is consistent with the recovery of initial rates by thermal treatment in inert streams and with the observed monotonic increase in CO oxidation selectivity as catalysts gradually approach steady-state CO coverages during reaction. Alkali appears to disrupt CO monolayer growth by promoting the formation of unreactive chemisorbed carbon via CO dissociation and disproportionation reactions, the rates of which increase when alkali is added to Pt surfaces. Chemisorbed carbon blocks some active Pt surface atoms, but also introduces obstacles that inhibit the formation of dense CO monolayers, thus retaining exposed Pt atoms required for the activation of O₂ co-reactants. Rb and Cs cations, which are more electropositive than Na cations, increase CO oxidation turnover rates more strongly, consistent with the proposed mechanisms for the electronic promotion effects of alkali on CO dissociation.

© 2005 Published by Elsevier Inc.

Keywords: Alkali promotion; H₂ spillover; CO oxidation

1. Introduction

H₂ is a useful energy carrier typically produced from fossil fuels. Its use in low-temperature fuel cells requires that impurities, specifically CO co-produced in reforming reactions, be removed, because they inhibit reactions at Pt an-

odes [1]. Selective oxidation of CO in H₂-rich streams is a potential route to achieving the required H₂ purity.

Supported Pt [2–6], Au [7–9], Cu [10], Pd [3], Ru [3,11], and Rh [3,12] catalyze selective CO oxidation in H₂-rich streams, but CO oxidation selectivities, based on the amount of O₂ used to form CO₂, are below 60%, even at low reaction temperatures (<500 K). Au/Co₃O₄ [7] and Au/MgO [13] have shown slightly higher selectivities (~70%); Mn, Mg, and Fe promoters increased selectivities on Au-based materials to ~80% [13,14]; Fe, Sn, and Ce [15–18] improved selectivities on Pt-based catalysts to similar levels. Pt-

* Corresponding author. Fax: +1-510-642-4778.

E-mail address: iglesia@cchem.berkeley.edu (E. Iglesia).

¹ Current address: Central Technical Research Laboratory, Nippon Oil Corporation, Yokohama 231-0815, Japan.

Fe/mordenite was recently reported to catalyze CO oxidation at 373 K with $\sim 100\%$ selectivity for reactants containing 98.5% H₂ [19]. Potassium added to Rh/SiO₂ and Rh/USY catalysts [20,21] led to a small increase in CO oxidation rates, but CO oxidation selectivities remained below 50% on all samples.

Supports affect many reactions involving H₂ [22–28], often via spillover processes, in which hydrogen adatoms are stabilized on support surfaces after H₂ dissociation on metal sites. Here we describe a ubiquitous connection between spillover and support-mediated H₂ oxidation pathways responsible for significant losses in CO oxidation selectivity. We also show that alkali modification of supports inhibits these spillover-mediated H₂ oxidation pathways and markedly increases CO oxidation selectivities on Pt-based catalysts in a manner reminiscent of the effects of alkali on hydrogenation and hydrogenolysis catalysis [29,30]. The use of Cs at surface densities between 0.8 and 6 Cs nm⁻² also led to a marked increase in CO oxidation turnover rates. CO oxidation turnover rates increased almost 10-fold when silica was modified with 1.6 Cs nm⁻² and CO oxidation selectivities increased concurrently from 63 to 90%. These improvements in CO oxidation rates and selectivities reflect (i) the titration of silanol groups by Cs with the consequent inhibition of spillover-mediated H₂ oxidation pathways, and (ii) a role of Cs in the formation of chemisorbed unreactive carbon species, which inhibit the growth of dense chemisorbed CO islands on the surface of Pt clusters.

2. Experimental

2.1. Catalyst synthesis and characterization

Pt/SiO₂ (1.6 wt%) was prepared by incipient wetness impregnation of SiO₂ (Syloid 222, Grace Davison, 228 m²/g; treated in ambient air at 773 K for 5 h) with aqueous solutions of Pt(NH₃)₄(NO₃)₂ (Aldrich; 99.995% purity). Impregnated samples were dried at 398 K for 12 h, then heated to 773 K at 0.0833 K s⁻¹ in ambient air, and held at 773 K for 5 h.

Alkali-promoted samples were prepared by impregnation of SiO₂ (treated as noted above) with aqueous solutions of cesium acetate (Aldrich; 99.9%) to give Cs surface densities between 0.8 and 6 Cs nm⁻². Samples were dried at 398 K and treated in ambient air at 773 K for 5 h (heating rate 0.0833 K s⁻¹). After this treatment, they were impregnated to incipient wetness with aqueous solutions of Pt(NH₃)₄(NO₃)₂ to give 1.6 wt% Pt/Cs–SiO₂ and treated in ambient air at 773 K for 5 h (heating rate 0.0833 K s⁻¹). The notation Cs-0.8 refers to a sample containing 1.6 wt% Pt and 0.8 Cs nm⁻² on SiO₂ (Table 1). Pt/Rb–SiO₂ and Pt/Na–SiO₂ (1.6 wt% Pt) catalysts with alkali contents of 1.6 alkali atoms/nm² were prepared by impregnation of SiO₂ with aqueous solutions of Rb or Na acetate (Aldrich; 99.8

Table 1
Fractional metal dispersion calculated from H₂ chemisorption

Promoter	Promoter loading (atoms/nm ²) ^a	Notation	Fractional Pt dispersion ^b
None	0	Pt/SiO ₂	0.13
Cs	0.8	Cs-0.8	0.16
	1.6	Cs-1.6	0.15
	2.5	Cs-2.5	0.26
	3.3	Cs-3.3	0.24
	4.8	Cs-4.8	0.23
	6.0	Cs-6.0	0.24
Rb	1.6	Rb-1.6	0.14
Na	1.6	Na-1.6	0.44

^a Per nm² total surface area measured by BET method.

^b Calculated from H₂ chemisorption, 308 K, 1:1 stoichiometry; 1.6 wt% Pt.

and 99.995%, respectively) by the same methods described above for Cs-containing samples.

Pt/Al₂O₃ (0.8 and 1.6 wt%) samples were prepared by incipient wetness impregnation of Al₂O₃ with aqueous solutions of H₂PtCl₆ · 6H₂O (Aldrich; Lot 10013LO, 99% purity). Impregnated Pt/Al₂O₃ samples were dried at 393 K in ambient air and treated in flowing dry air (Airgas, UHP, 1.2 cm³/(g s)); the temperature was increased to 873 K at 0.167 K s⁻¹ and held at 873 K for 5 h. We prepared Al₂O₃ (160 m² g⁻¹) by treating Al(OH)₃ (Aldrich) in flowing dry air (Airgas, UHP, 1.2 cm³/(g s)), increasing the temperature to 923 K at 0.167 K s⁻¹, and holding at 923 K for 5 h; this procedure led to the formation of γ -Al₂O₃ (160 m² g⁻¹) [31]. All samples were sieved to retain particles with a 0.18–0.36-mm diameter.

Pt dispersion was measured from volumetric H₂ chemisorption uptakes at 308 K with a Quantasorb chemisorption analyzer (Quantachrome Corp.) assuming a 1:1 H/Pt adsorption stoichiometry [32]. Catalysts were treated in H₂ at 623 K for 2 h and then evacuated at 623 K for 0.5 h before chemisorption measurements. After treatment at 623 K, the samples were cooled to 308 K and H₂ chemisorption isotherms were measured at 5–50 kPa H₂; we also measured a backdesorption isotherm by repeating this procedure after evacuating the sample at 308 K for 0.33 h. These two isotherms were extrapolated to zero H₂ pressure, and their difference was defined as strongly chemisorbed hydrogen and used to calculate Pt dispersions. Accurate measurements required at least 0.4-g samples, thus precluding H₂ chemisorption measurements after reaction on the small catalyst amounts (<0.1 g) used for reactions.

2.2. Catalytic reaction rates and selectivities

CO oxidation reaction rates and selectivities were measured at 383 K with a packed-bed reactor with plug-flow hydrodynamics. Pt/Al₂O₃ (0.020 g), Pt/SiO₂ (0.10 g), and Pt/alkali–SiO₂ (0.020 g) samples were diluted with 0.5 g of acid-washed quartz powder (Aldrich; 0.25–0.43 mm) to prevent temperature gradients and treated in H₂ (Praxair,

UHP, $4 \text{ cm}^3/(\text{g s})$) with heating to 623 K at 0.133 K s^{-1} ; this temperature was maintained for 2 h. Samples were then cooled to 383 K in H_2 , and reactants were introduced at residence times corresponding to total flow rates of 1.0, 0.67, or $0.33 \text{ cm}^3 \text{ s}^{-1}$ in a mixture containing 1 kPa CO, 1 kPa O_2 , 70 kPa H_2 , and balance He (Praxair). Reactant and product concentrations were measured by on-line gas chromatography (Hewlett–Packard; model 5890) with a packed column (Alltech; Porapak R 80–100 mesh) and flame ionization and thermal conductivity detectors. CH_4 was not detected among the reaction products under any conditions. CO oxidation selectivity is defined as the percentage of the O_2 converted appearing as CO_2 [2,6,15,16]. H_2 oxidation rates were estimated from the difference between measured CO and O_2 conversion rates [16].

Reaction rates and selectivities were also measured in a recirculating batch reactor [33] after treatment of samples in H_2 (Airgas, UHP, $4 \text{ cm}^3/(\text{g s})$) at 623 K for 2 h. The recirculating reactor (520 cm^3) was evacuated to $<0.1 \text{ Pa}$ before the introduction of reactants (1 kPa CO, 1 kPa O_2 , 70 kPa H_2 , balance He). A graphite gear micropump was used to recirculate the reactor contents (at $>2 \text{ cm}^3/\text{s}$) and to ensure low conversions per pass ($<1\%$) [34]. Reactant and product concentrations were measured by on-line gas chromatography (Hewlett–Packard; model 5890) with a packed column (Alltech; Porapak R 80–100 mesh) and a thermal conductivity detector; gas samples were extracted from the circulating stream with an automated sampling valve placed within the recirculation loop.

2.3. Infrared spectra measurement

Infrared spectra of adsorbed CO were measured at 303 K with a Mattson RS-1000 infrared spectrometer in transmission mode (2 cm^{-1} resolution) and an in situ flow cell with CaF_2 windows. The temperature was held constant with a resistive heater and a temperature controller (Watlow; series 982). We prepared self-supported wafers (13-mm diameter) by pressing samples (0.015 g) at 60 MPa and treated these samples in H_2 at 623 K for 2 h before cooling them to 303 K in He and exposing them to CO. A background spectrum was collected, and spectra were then acquired for a period of time (0.06–3.6 ks) after exposure to 1 kPa CO/He at 303 K. We corrected spectra for gas-phase CO by subtracting spectra collected at each CO pressure without a sample wafer. We probed for alkali effects on silanol surface densities by measuring the intensity of SiO–H stretching bands as a function of Cs content. Samples were treated in He at 623 K and cooled to 323 K before these measurements.

Infrared spectra were also measured during reactions of O_2 with H_2 –CO mixtures in diffuse–reflectance mode with a reflectance attachment (Harrick Scientific; DPR: XXX) and an in situ cell (HVC-DR2) at a resolution of 8 cm^{-1} . Powder samples were placed on a porous disk, through which reactants were introduced. We collected in situ infrared spectra during catalytic reactions of H_2 –CO– O_2 mixtures by first

treating samples in H_2 as described above, cooling them to 383 K to collect background spectra, exposing them to reactant mixtures (1 kPa CO, 1 kPa O_2 , 70 kPa H_2 , balance He) at 383 K, and acquiring spectra at times on stream between 0.06 and 3.6 ks. Reflectance data were converted to pseudo-absorbance with the use of the Kubelka–Munk formalism [35].

3. Results and discussion

3.1. Metal dispersion in supported Pt catalysts

Metal dispersions are listed in Table 1 for all samples. Pt dispersions increased slightly with increasing Cs surface density (0 to 2.5 atoms/nm^2) but remained constant at higher Cs surface densities. At 1.6 Cs nm^{-2} , Cs and Rb modifications of SiO_2 gave similar Pt dispersions, but Na-modified SiO_2 gave significantly higher values. Alkali has previously been reported to increase metal dispersions [36–39], without rigorous mechanistic interpretations. Alkali increases the zero-point of charge of SiO_2 surfaces from a pH of 3.2–4.1 [40–43] to ~ 8 [40]; thus, cationic Pt ammine complexes (solution pH ~ 5) should interact more strongly with unmodified SiO_2 surfaces, but instead we find lower dispersions for these samples. Thus, electrostatic arguments do not account for the higher metal dispersions achieved on alkali-modified SiO_2 , the underlying basis for which remains unclear.

3.2. Mechanistic analysis of the oxidation of CO– H_2 mixtures on supported Pt

Fig. 1a shows CO, O_2 , and H_2 conversions and CO oxidation selectivities on 1.6 wt% Pt/ Al_2O_3 as a function of contact time at 393 K in a gradientless batch reactor; this reactor allows detailed studies of the effects of contact time and of CO and O_2 reactant depletion on CO oxidation rates and selectivities. CO conversion increased with contact time and reached 100% at $\sim 6 \text{ ks}$ (Fig. 1a). H_2 conversion gradually increased with contact time and then increased sharply as all residual O_2 reacted rapidly with H_2 after CO was depleted. CO oxidation selectivities decreased only slightly (from 53 to 46%) with increasing contact time as CO partial pressures decreased concurrently from 1 kPa to essentially zero, and then decreased sharply as all remaining O_2 was used to combust H_2 ; such a weak dependence of CO selectivity on CO pressure is surprising in view of the expected inhibition of H_2 oxidation steps by co-adsorbed CO [44].

We consider first a Langmuir-type mechanism [4,6,15] to describe measured H_2 and CO oxidation rates and the observed effects of contact time. CO is assumed to adsorb reversibly, since surface residence times of chemisorbed CO are much shorter than characteristic times for their reaction with chemisorbed oxygen to give CO_2 at conditions similar to those we have used here [4]. H_2 adsorbs more weakly than CO in quasi-equilibrated steps on Pt surfaces.

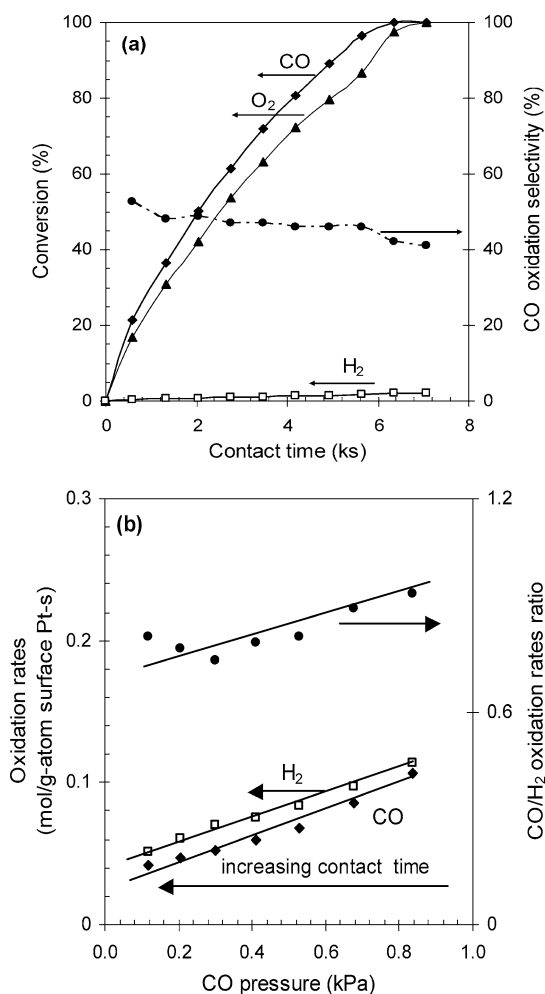
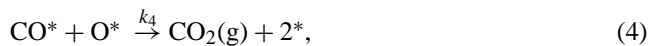


Fig. 1. (a) CO (◆), O₂ (▲), and H₂ (□) conversions and CO oxidation selectivity (●) vs contact time, (b) CO (◆) and H₂ (□) oxidation rates and CO/H₂ oxidation rates ratio (●) vs the residual CO concentration during selective CO oxidation reaction on 1.6 wt% Pt/Al₂O₃ in a gradientless batch reactor (0.030 g catalyst, 393 K, 1 kPa CO, 1 kPa O₂, 70 kPa H₂, balance He). Rates were calculated from the local slope between two sequential conversions.

Adsorbed dioxygen desorbs below 200 K on Pt surfaces, but chemisorbed oxygen atoms desorb only above 650 K [45]. Thus, we assume quasi-equilibrated molecular adsorption and irreversible dissociative chemisorption. Surface reactions of CO* are assumed to be irreversible in view of the favorable thermodynamics of the overall reaction ($\Delta G^0 = -316$ kJ/mol). CO oxidation rates were not influenced by the presence of H₂O under our reaction conditions; thus, H₂O desorption and oxidation of adsorbed hydrogen either are irreversible or proceed via reactions of minority adsorbed intermediates.

These elementary steps are as follows (* stands for exposed Pt surface atoms):



These assumptions lead to a CO/H₂ oxidation rate ratio (R) given by

$$R = \frac{r_{\text{CO}}}{r_{\text{H}_2}} = \frac{k_4 K_1 [\text{CO}]}{k_6 \sqrt{K_5} [\text{H}_2]} \quad (8)$$

and to individual CO and H₂ oxidation turnover rates (r_{CO} and r_{H_2}) given by

$$r_{\text{CO}} = \frac{r'_{\text{CO}}}{[\text{L}]} = \frac{2k_3 k_4 K_2 [\text{O}_2]}{K_1 [\text{CO}] (k_4 K_1 [\text{CO}] + k_6 \sqrt{K_5} [\text{H}_2])}, \quad (9)$$

$$r_{\text{H}_2} = \frac{r'_{\text{H}_2}}{[\text{L}]} = \frac{2k_3 k_6 K_2 [\text{O}_2] \sqrt{K_5} [\text{H}_2]}{K_1^2 [\text{CO}]^2 (k_4 K_1 [\text{CO}] + k_6 \sqrt{K_5} [\text{H}_2])}, \quad (10)$$

where [L] is the concentration of active sites and is about equal to the number of adsorbed CO* under most of our reaction conditions. CO oxidation selectivities (S_{CO}) are related to the oxidation rate ratio (R) by

$$\frac{1}{S_{\text{CO}}} = \frac{r_{\text{CO}} + r_{\text{H}_2}}{r_{\text{CO}}} = \frac{1}{R} + 1. \quad (11)$$

Fig. 1b shows relative (R) and individual oxidation rates of H₂ and CO (r_{H_2} and r_{CO}) as a function of residual CO concentration. Rates are measured from the local slope of CO and O₂ concentrations versus contact time. H₂ co-reactants were present in large excess, and thus H₂ partial pressures remained essentially unchanged with increasing contact time until CO conversions neared 100% and the remaining H₂ rapidly formed H₂O.

The proposed elementary steps predict that R decreases linearly as the residual CO concentration decreases (with increasing contact time) and ultimately approaches a value of zero (Eq. (8)), in contrast with the weaker effects and positive intercept shown in Fig. 1b. Moreover, r_{H_2} actually decreased with time, instead of increasing as the CO concentration concurrently decreased, as expected from the negative order in CO for r_{H_2} in Eq. (10). Thus, the data in Fig. 1 are inconsistent with competitive monofunctional pathways of CO and H₂ oxidation on Pt surfaces; they reflect instead parallel H₂ oxidation pathways on catalytic sites that do not adsorb CO.

3.3. Effect of support on H₂ oxidation via spillover

The ability of Pt/Al₂O₃ catalysts to spill hydrogen atoms formed via H₂ dissociation on Pt sites spillover onto binding sites on Al₂O₃ [22–29] led us to consider paths involving such species, the concentration of which may be unaffected

Table 2

Effect of support on oxidation rates (r_{CO} , r_{H_2}) and selectivities (S_{CO}) on Pt/Al₂O₃, Pt/SiO₂ and Pt/Cs–SiO₂ (Cs-1.6) catalysts during CO oxidation in the presence of H₂ in a gradientless batch reactor (1 kPa CO, 1 kPa O₂, 70 kPa H₂, balance He, CO conversion ~20%)

Sample	r_{CO} (10 ⁻² mol/ (g-atom-surface-Pt s))	r_{H_2} (10 ⁻² mol/ (g-atom-surface-Pt s))	S_{CO} (%)	$r_{\text{CO}}/r_{\text{H}_2}$ (R)
0.8 wt% Pt/Al ₂ O ₃ ^a	18	20	47	0.89
0.8 wt% Pt/Al ₂ O ₃ + Al ₂ O ₃ loose mixture ^{a, b}	21	26	44	0.80
0.8 wt% Pt/Al ₂ O ₃ + Al ₂ O ₃ intimate mixture ^{a, b}	22	37	37	0.59
1.6 wt% Pt/Al ₂ O ₃ ^c	1.9	1.2	61	1.6
1.6 wt% Pt/SiO ₂ ^c	1.5	0.56	73	2.6
Cs-1.6 ^c	10.7	0.85	93	12.5

^a Reaction temperature was 403 K.

^b Physical mixtures of 0.02 g of Pt/Al₂O₃ catalyst and 0.1 g of pure Al₂O₃. Particles sieved to 180–355 μm.

^c Reaction temperature was 363 K.

by CO co-adsorption. Such spillover-mediated routes require Pt clusters only for H₂ dissociation, a step that is fast and quasi-equilibrated, even on Pt surfaces predominantly covered by CO.

Sinfelt and Lucchesi [22] proposed that spillover hydrogen was involved in ethene hydrogenation. Reaction rates increased when Al₂O₃ was present even in physical mixtures, and rates were significantly higher when Pt clusters were supported on Al₂O₃ instead of SiO₂. Similar support effects were reported for CO hydrogenation on supported Pt clusters [23,24]. McVicker and Vannice [30] reported that SiO₂ modified by K led to lower CO hydrogenation rates on supported Fe catalysts. Miller et al. [29] showed that alkane hydrogenolysis turnover rates were higher on Pt/Al₂O₃ (0.62 s⁻¹) than on Pt/SiO₂ (0.19 s⁻¹) and that addition of K to SiO₂ or zeolites inhibits hydrogenolysis by suppressing hydrogen spillover. The addition of Cs and Na to SiO₂ was shown to inhibit hydrogen spillover on Ru/SiO₂ [46]. Thus, it appears that spillover hydrogen is a reactive species and that alkali titrates sites required to stabilize such species on supports.

We examined support effects on CO oxidation rates and selectivities in H₂-rich mixtures by comparing Pt/Al₂O₃ and Pt/SiO₂, as well as physical mixtures of Pt/Al₂O₃ (0.02 g) with pure Al₂O₃ (0.10 g), as loose mixtures of their respective agglomerates (0.18–0.36 mm) and as intimate mixtures formed by grinding of catalysts and pure supports together and re-forming of agglomerates. Tables 2 and 3 show r_{CO} , r_{H_2} , R , and S_{CO} at two CO conversion levels (~20 and ~70%) on these samples. The effects of the identity and

Table 3

Effect of support on oxidation rates (r_{CO} , r_{H_2}) and selectivities (S_{CO}) on Pt/Al₂O₃, Pt/SiO₂ and Pt/Cs–SiO₂ (Cs-1.6) catalysts during CO oxidation in the presence of H₂ in a gradientless batch reactor (1 kPa CO, 1 kPa O₂, 70 kPa H₂, balance He, CO conversion ~70%)

Sample	r_{CO} (10 ⁻² mol/ (g-atom-surface-Pt s))	r_{H_2} (10 ⁻² mol/ (g-atom-surface-Pt s))	S_{CO} (%)	$r_{\text{CO}}/r_{\text{H}_2}$ (R)
0.8 wt% Pt/Al ₂ O ₃ ^a	8.1	9.2	48	0.88
0.8 wt% Pt/Al ₂ O ₃ + Al ₂ O ₃ loose mixture ^{a, b}	6.2	10.2	37	0.60
0.8 wt% Pt/Al ₂ O ₃ + Al ₂ O ₃ intimate mixture ^{a, b}	7.3	14.9	32	0.49
1.6 wt% Pt/Al ₂ O ₃ ^c	0.79	0.76	51	1.0
1.6 wt% Pt/SiO ₂ ^c	0.55	0.32	63	1.7
Cs-1.6 ^c	6.1	0.90	87	6.8

^a Reaction temperature was 403 K.

^b Physical mixtures of 0.02 g of Pt/Al₂O₃ catalyst and 0.1 g of pure Al₂O₃. Particles sieved to 180–355 μm.

^c Reaction temperature was 363 K.

amount of the support were similar at these two conversion levels. Turnover rates (per exposed Pt) for CO oxidation on 0.8% Pt/Al₂O₃ were not influenced by additional amounts of pure Al₂O₃, but H₂ oxidation rates increased with increasing amounts of Al₂O₃ in physical mixtures; these effects became stronger when Al₂O₃ was intimately mixed with Pt/Al₂O₃. Thus, Al₂O₃ supports, even as loose physical mixtures, led to higher H₂ oxidation rates, even though Al₂O₃ did not catalyze H₂ oxidation in the absence of Pt clusters. This suggests a synergy between Pt clusters, required for H₂ dissociation, and Al₂O₃ supports, which catalyze H₂ oxidation even when Pt and support functions reside at distances (0.01–0.10 mm) much larger than atomic dimensions. These pathways account for a significant fraction of the unselective O₂ conversion pathways detected during oxidation of CO in H₂-rich mixtures. Support sites do not interact strongly with CO; thus, spillover pathways also account for the weak effects of CO on the relative rates of CO and H₂ oxidation. These data and conclusions imply that monofunctional CO oxidation pathways on Pt surfaces are in fact much more selective than previously inferred from CO oxidation data reported for Pt/Al₂O₃ catalysts.

In light of these findings, we examined SiO₂ as a support, because it is less effective than Al₂O₃ in stabilizing spillover hydrogen [29]. At 20% CO conversion, Pt/SiO₂ (1.6 wt%) gave a lower r_{H_2} (0.0056 s⁻¹) than 1.6 wt% Pt/Al₂O₃ (0.012 s⁻¹) (Table 2). Pt dispersions are similar in these two catalysts (16 and 22%, respectively); thus, cluster size effects do not account for these different values of r_{H_2} . In contrast, r_{CO} was essentially unaffected by support

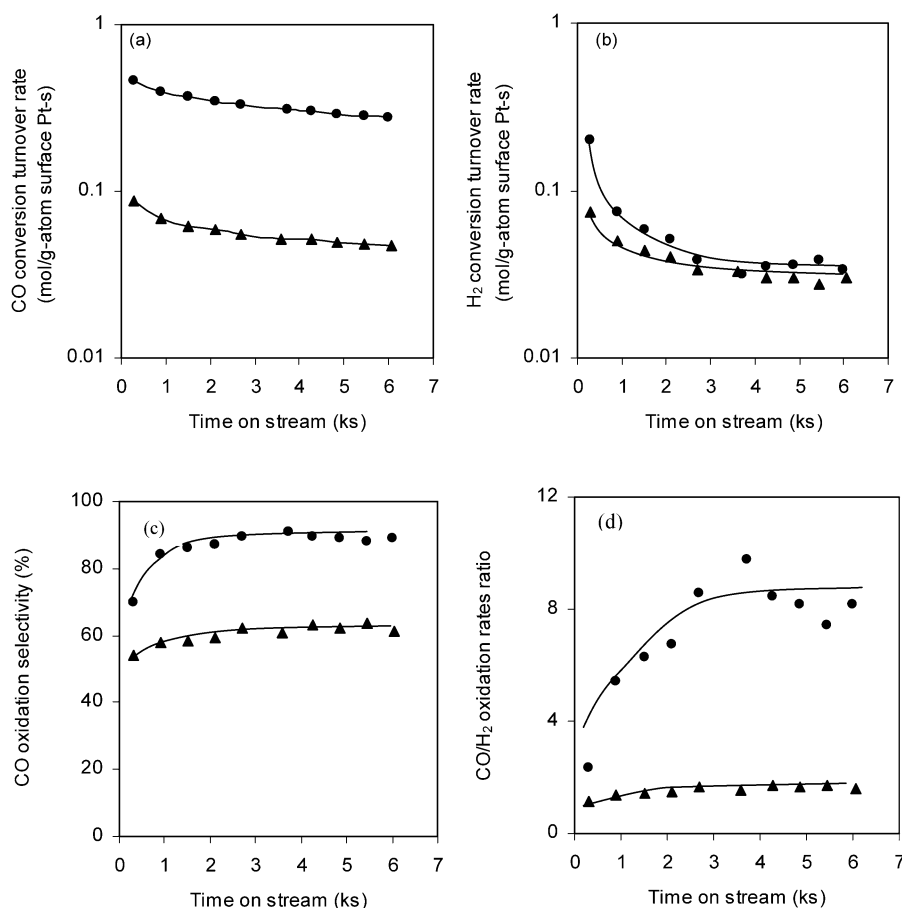


Fig. 2. (a) CO oxidation rate, (b) H₂ oxidation rate, (c) CO oxidation selectivity and (d) ratio of CO to H₂ oxidation rates of Pt/SiO₂ (▲) and Cs-1.6 (●) in a packed-bed flow reactor (0.100 g Pt/SiO₂ and 0.020 g Cs-1.6 diluted with 0.5 g acid-washed quartz, 383 K, 1 kPa CO, 1 kPa O₂, 70 kPa H₂, balance He, total flow 0.67 cm³/s).

(0.015 vs 0.019 s⁻¹). As a result, S_{CO} and R were higher on 1.6 wt% Pt/SiO₂ (73%, 2.6) than on 1.6 wt% Pt/Al₂O₃ (61%, 1.6). These conclusions are similar when catalytic data are compared at higher CO conversions (70%; Table 3).

3.4. Effect of Cs on CO oxidation rate and selectivity on Pt/SiO₂

The systematic addition of alkali to Pt/SiO₂ is considered next in an effort to inhibit residual contributions from spillover-mediated H₂ oxidation pathways on SiO₂. Oxidation rates r_{CO} and r_{H_2} , R , and S_{CO} for 1.6 wt% Pt/Cs–SiO₂ (1.6 Cs nm⁻²) at two conversion levels (~20 and ~70% CO) are listed in Tables 2 and 3. The addition of Cs to SiO₂ supports led to catalysts with higher CO oxidation selectivities and, unexpectedly, to much higher CO and H₂ oxidation turnover rates. CO oxidation turnover rates on Pt/Cs–SiO₂ (1.6 Cs nm⁻²) were about 10 times larger than those on Pt/SiO₂.

Fig. 2 shows r_{CO} , r_{H_2} , S_{CO} , and R as a function of time on stream on Cs-1.6 and Pt/SiO₂ in a packed-bed reactor with plug-flow hydrodynamics. CO oxidation turnover rates decreased slightly with time and reached near-constant val-

ues after ~4 ks; these steady-state values were ~7 times larger on Cs-1.6 than on Pt/SiO₂. S_{CO} increased with time on stream and then reached steady-state values; these values were significantly higher on Cs-1.6 than on Pt/SiO₂ (90 vs 63%). H₂ oxidation rates were also higher on Cs-1.6 than on Pt/SiO₂ during the first 1 ks, but then reached similar values (0.03 mol/(g-atom-surface-Pt-s)) after ~3 ks. This decrease in r_{H_2} with time is more pronounced than that observed for r_{CO} on Cs-1.6; as a result, S_{CO} and R increased sharply with time. The oxidation rate ratio (R) increased by a factor of 4 over 3 ks on Cs-1.6, but only by a factor of ~1.4 on Pt/SiO₂.

In order to explain the behavior of Cs-modified catalysts, we first confirmed that reaction products reflect predominantly Pt-catalyzed pathways, without significant contributions from spillover-mediated H₂ oxidation. Thus, CO oxidation selectivities should be greater on Cs-modified samples, but also more sensitive to CO partial pressure and surface coverage. Detailed kinetic studies in a recirculating reactor showed that CO/H₂ oxidation rate ratios (R) do indeed reflect predominantly Pt-catalyzed reactions on Cs-1.6 samples with minimal contributions from spillover-mediated H₂ oxidation on support surfaces. Rates were measured from the local derivative of CO and H₂ oxidation

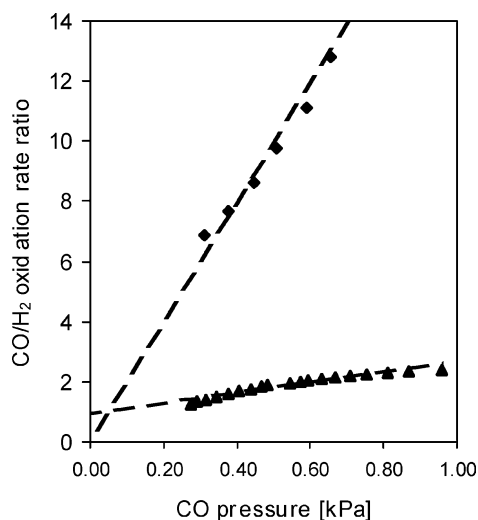


Fig. 3. CO/H₂ oxidation rates ratios vs residual CO concentration during selective CO oxidation on Cs-1.6 (■) and 1.6 wt% Pt/SiO₂ (▲) in a gradientless batch reactor (0.072 g Pt/SiO₂ and 0.026 g Cs-1.6, 363 K, 1 kPa CO, 1 kPa O₂, 70 kPa H₂, balance He). Oxidation rates were determined from the derivative of a quadratic fit of batch reactor conversions as function of contact time, for CO conversions below 70%.

turnovers with time for CO conversions below 70% in this batch reactor. Fig. 3 shows a sharp, linear decrease in R with decreasing CO concentration (increasing contact time) and a zero intercept for Cs-1.6, as predicted by Eq. (8). In contrast, a smaller change and a positive intercept are observed on Pt/SiO₂. Thus, H₂ oxidation pathways requiring spilled-over hydrogen appear to make minimal contributions to H₂O formation rates on Cs-1.6 but contribute significantly to the products observed on Pt/SiO₂. Only on Cs-1.6 is the rate ratio accurately described by the Langmuir-type monofunctional oxidation mechanism proposed in Section 3.2.

3.5. Effect of Cs on spillover pathways for H₂ oxidation

The addition of Cs to SiO₂ supports led to a marked increase in S_{CO} at all Cs surface densities (0.8–6 Cs nm⁻²) (Fig. 4). Cs increased both r_{CO} and r_{H_2} , but its effect was stronger on r_{CO} , which led to increasing values of S_{CO} with increasing Cs surface density up to 1.6 Cs nm⁻² and a constant S_{CO} of ~90% at higher Cs surface densities. These effects reflect inhibition and ultimate suppression of spillover-mediated H₂ oxidation pathways as Cs surface densities increased on SiO₂ supports. Above 2.5 Cs nm⁻², catalytic selectivities reflected predominantly Pt-catalyzed H₂ oxidation pathways and exhibited the inhibition with increasing CO pressure and surface coverage that is characteristic of Pt surfaces. Thus, higher Cs contents did not influence selectivities.

Here, we provide evidence for the role and location of alkali on support surfaces and for their specific involvement in the titration of silanol groups, which appear to stabilize

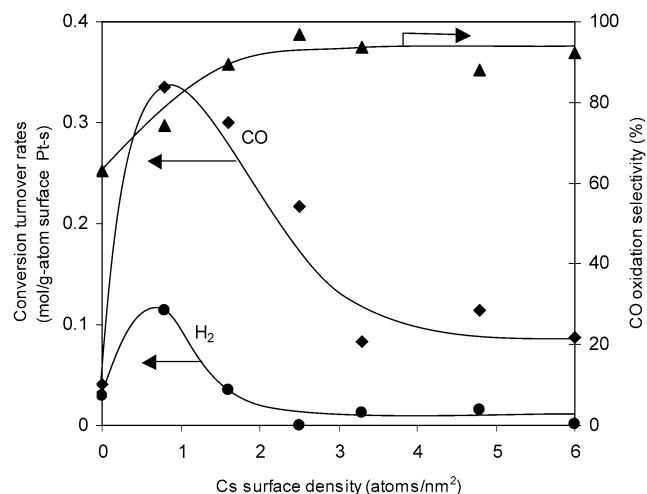


Fig. 4. Effects of Cs surface density on Pt/SiO₂ on CO (◆) and H₂ (●) conversion turnover rates and CO₂ selectivity (▲) during selective CO oxidation in a packed-bed flow reactor. Oxidation rates and selectivities given when the ratio of CO to H₂ oxidation rates reached steady-state value, after ~4.2 ks on stream (0.100 g Pt/SiO₂ and 0.020 g Cs-samples were diluted with 0.5 g acid-washed quartz, 383 K, 1 kPa CO, 1 kPa O₂, 70 kPa H₂, balance He, total flow rate 0.67 cm³/s).

spillover hydrogen [29,46]. Partial dehydroxylation by thermal treatment [47,48] and titration by alkali [29,46] have been reported to inhibit hydrogen spillover. Infrared spectra in the O–H stretching region were measured [49] as a function of Cs content to probe the titration of SiO–H groups to form SiO–Cs.

Fig. 5 shows infrared spectra in the O–H stretching region for Pt/SiO₂ samples with Cs surface densities of 0–4.8 Cs/nm². The silanol stretching modes appear at 3800–3200 cm⁻¹; the narrow band at 3750 cm⁻¹ corresponds to isolated silanols, and broader bands at 3700–3400 cm⁻¹ arise from hydrogen-bonded vicinal OH groups. All SiO–H bands became weaker as the Cs surface density increased, consistent with their replacement by SiO–Cs species during contact with aqueous Cs⁺ cations. Fig. 6 shows total integrated OH intensities, with the band at 2100–1750 cm⁻¹ for the SiO₂ framework [49] as an internal standard, as a function of the Cs surface density. These data show that titration of OH groups increased monotonically with Cs content. At Cs surface densities of 0.8 Cs nm⁻², ~65% of the silanols in Pt/SiO₂ were titrated; Si–OH bands essentially disappeared at 4.5 Cs nm⁻².

The intensities for silanol bands and the corresponding S_{CO} values are shown for each sample in Fig. 6 as a function of Cs surface density. S_{CO} increased from 63 to 92% as OH groups were titrated by Cs and reached constant values when ~85% of the silanol groups were titrated. These data are consistent with inhibition of spillover-mediated H₂ oxidation pathways upon titration of silanols by Cs. We conclude that alkali influences selectivity by suppressing these pathways and that monofunctional oxidation of H₂–CO mixtures (70:1 molar ratio) occurs on Pt with selectivity greater than 90%, until CO is depleted, at which point H₂ rapidly

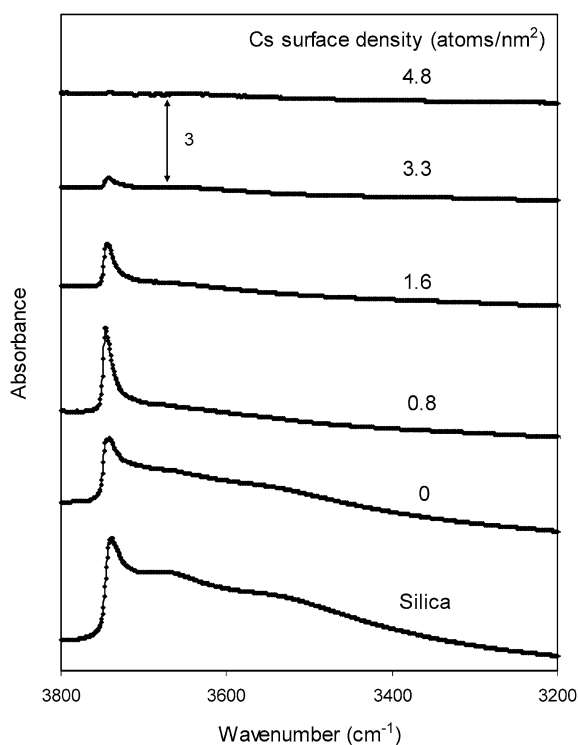


Fig. 5. Infrared spectra of silica, Pt/SiO₂ and Cs-promoted catalysts at 323 K in He flow after treatment in He at 623 K for 0.9 ks. Spectra normalized by the intensity of the Si–O–Si band.

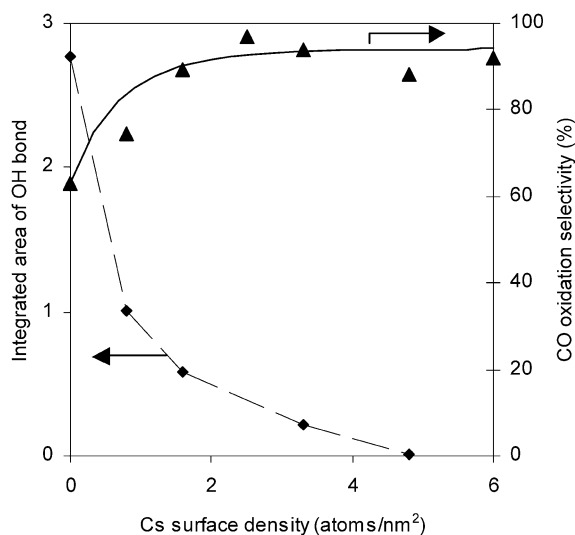


Fig. 6. Changes in the integrated area of surface silanols (◆) and CO oxidation selectivity (▲) as a function of Cs surface density. Infrared spectra were taken at 323 K in He flow after treatment in He at 623 K for 0.9 ks. Surface silanols normalized by the area of the Si–O–Si band. Selectivities given when the ratio of CO to H₂ oxidation rates reached steady-state value, after ~4.2 ks on stream (0.100 g Pt/SiO₂ and 0.020 g Cs-samples diluted with 0.5 g acid-washed quartz, 383 K, 1 kPa CO, 1 kPa O₂, 70 kPa H₂, balance He, total flow rate 0.67 cm³ s⁻¹).

consumes all of the remaining O₂. Next, we discuss these monofunctional CO and H₂ oxidation pathways on Pt and how they are affected by alkali modification.

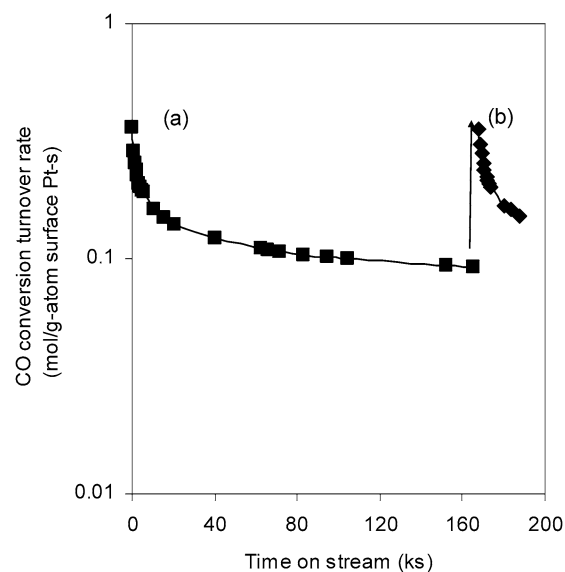


Fig. 7. (a) CO oxidation rate following standard reduction pretreatment and (b) after regeneration in He at 623 K for Cs-2.5 in a packed-bed flow reactor (0.020 g catalyst diluted with 0.5 g acid-washed quartz, 383 K, 1 kPa CO, 1 kPa O₂, 70 kPa H₂, balance He, total flow rate 0.34 cm³/s).

3.6. Deactivation behavior during catalytic oxidation of H₂–CO mixtures

In the following paragraphs, changes in the intrinsic behavior of Pt surfaces will be discussed as a function of time on stream and of Cs surface density. CO oxidation rates decreased with time over ~48 h (Fig. 7) and CO oxidation selectivities increased concurrently (e.g., Fig. 2). Initial reaction rates and selectivities were restored simply by treating samples in He flow at 623 K for 0.9 ks. Thus, the observed decrease in reaction rates and the concurrent increase in selectivity with time on stream do not reflect sintering or oxidation of Pt clusters or a decrease in the number of active sites caused by unreactive unsaturated deposits, because such processes would not be reversed by treatment with an inert gas at relatively low temperatures. The only other possibility is that a gradual increase in chemisorbed CO coverages to their steady-state value accounts for the observed catalyst deactivation and that CO desorption restores initial oxidation rates and selectivities.

Changes in the concentration of species adsorbed on Pt crystallites were probed by measurement of the infrared spectra of chemisorbed carbonyl species [50–54] at ambient temperatures and during catalytic oxidation of H₂–CO mixtures at 383 K. In situ diffuse-reflectance spectra were measured on Cs-1.6 as a function of time on stream, concurrently with CO oxidation rate measurements. Fig. 8 shows that the intensity of the infrared band centered near 2056 cm⁻¹, corresponding to stretching vibrations of linearly adsorbed CO, increased with time on stream, in parallel with a decrease in CO oxidation rates. After steady state was reached, increasing the CO partial pressure did not change the concentration of adsorbed CO, but led to a decrease in r_{CO} , consistent with

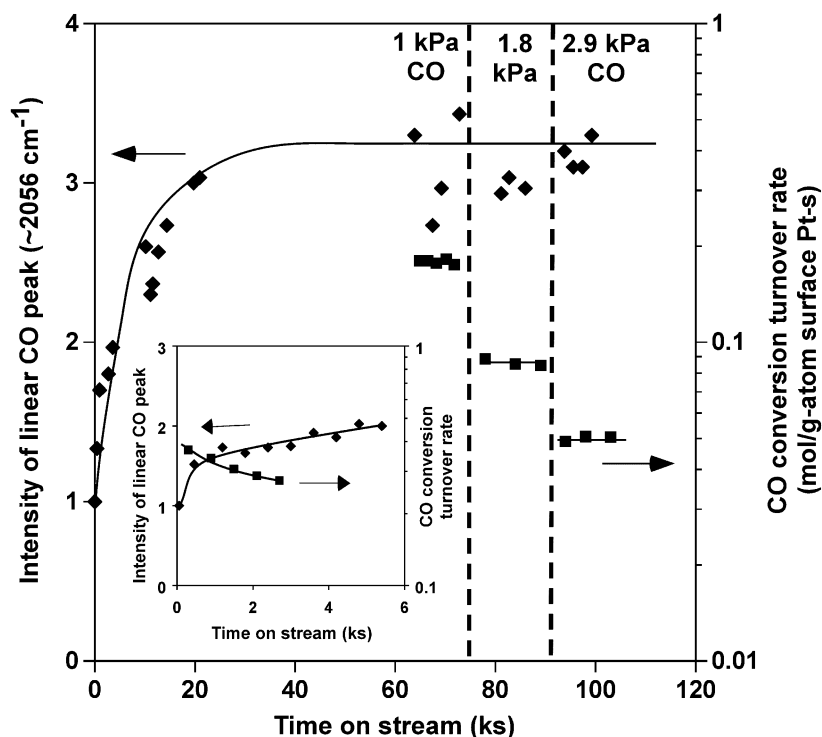


Fig. 8. Simultaneous measurement of CO oxidation rate (■) and intensity of the linear adsorbed CO peak (◆) as function of time on stream using a diffuse reflectance cell for Cs-1.6 catalyst (383 K, 1 kPa CO, 1 kPa O₂, 70 kPa H₂ balance He, total flow 0.67 cm³/s). CO partial pressure was increased (1.8 kPa, 2.9 kPa) independently of other gases. Inset shows CO oxidation rate and infrared band intensities at short times.

the proposed Langmuir-type mechanism, which requires a surface nearly covered with the most abundant reactive intermediate, adsorbed CO. In this mechanism, reaction rates decreased as the concentration of chemisorbed CO increased because of the consequent gradual loss of free sites required to adsorb and dissociate required O₂ co-reactants. These conclusions are consistent with recent studies of selective CO oxidation in H₂ on Pt/Al₂O₃ using isotopic jump methods, which showed that the amount of reversibly adsorbed CO actually increased during “deactivation” [4].

The kinetic consequences of an increase in adsorbed CO to its steady-state coverage are equivalent to those of a gradual increase in the CO adsorption constant (K_1) with time. In Figs. 2 and 8, r_{CO} and r_{H_2} decrease with time and the effective value of K_1 (proportional to the concentration of adsorbed CO) increases, consistent with Eqs. (9) and (10). Eq. (8) predicts that R is proportional to K_1 and is expected to increase with time, as observed experimentally (Fig. 2). Although the correlation between adsorbed CO and the observed changes in r_{CO} is clear from these data, the reasons for the extremely slow increase in CO surface concentration with time are less evident, because quasi-equilibrated CO chemisorption steps should lead to constant coverages within typical turnover times (~ 30 s), but steady-state chemisorbed CO concentrations and CO oxidation turnover rates appear to require significantly longer times (~ 40 ks).

CO chemisorbs together with O₂ or H₂ to form stable, dense, segregated islands [55–70], but initial contact be-

tween Pt surfaces and CO–O₂–H₂ mixtures would lead to relative coverages that reflect the sticking coefficient of each molecule, instead of their steady-state or equilibrium endpoint. Such initial adsorbed configurations evolve into dense islands that minimize repulsive interactions between CO* and O* species. Strongly bound O* atoms interfere with the growth of these chemisorbed CO islands over extended cluster surfaces. CO oxidation turnovers gradually deplete O*, forming free sites that can be titrated by CO* [55] in a process that decreases the density of O* and H* and the rates of both CO and H₂ oxidation turnovers. This process reflects the approach of CO and H₂ oxidation reactions to their steady-state instead of deactivation of the catalytic materials.

CO rapidly forms dense monolayers on Pt in the absence of competitive co-adsorption of other molecules; subsequent contact with H₂ or O₂ does not disrupt such structures at low temperatures [57,60,62,71]. In the kinetic formalism described above, the catalytic behavior of clean Pt surfaces pretreated with CO reflects true values of K_1 , and thus they exhibit lower, but stable, CO and H₂ oxidation rates. Treatment in CO for 1 h at 453 K [55] or 363 K [16] before CO oxidation at the respective catalytic temperatures eliminated initial rate transients in previous studies. In the present study, pre-adsorption of CO (1 kPa) on Cs-2.5 at 383 K for 1 h before H₂–CO–O₂ reactions led to lower initial r_{CO} (Fig. 9a) and higher values of R (Fig. 9b), but r_{CO} still decreased slightly with reaction time. This appears to reflect the immediate formation of unreactive chemisorbed carbon (C*) upon

contact with CO on Cs-modified catalysts, which disrupts monolayer growth, consistent with the gradual approach to steady-state rates, and irreversibly blocks active Pt surface atoms, as discussed below.

3.7. Effect of alkali on Pt-catalyzed CO and H₂ oxidation pathways

The inhibition of CO monolayer growth by chemisorbed carbon, as occurs on Cs-containing catalysts, would lead to higher turnover rates when rates are rigorously normalized by the number of exposed Pt atoms available during reaction.

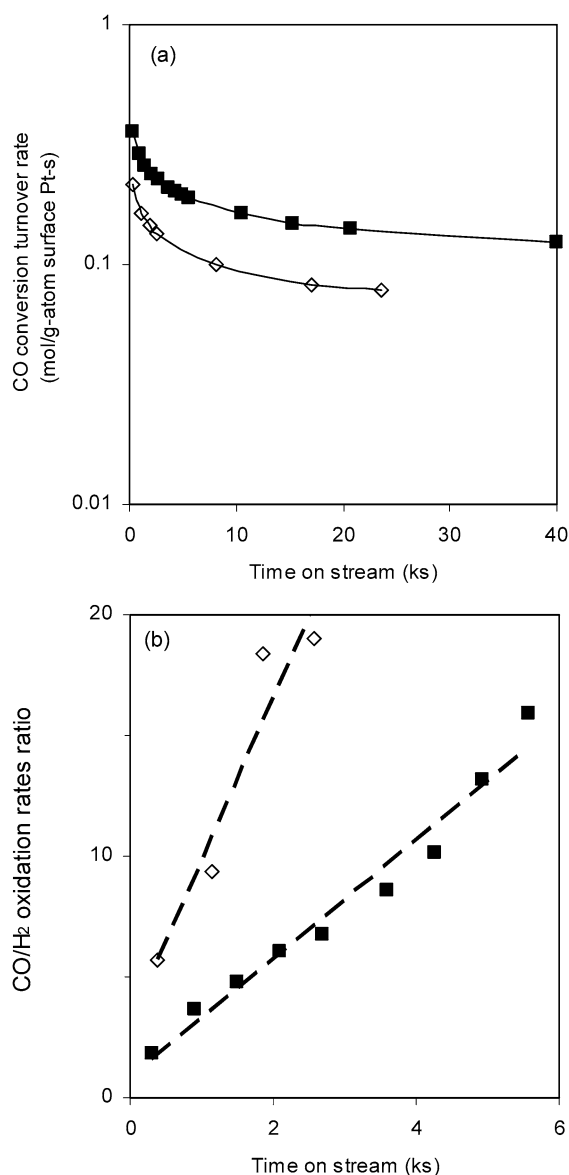


Fig. 9. (a) CO oxidation rates and (b) CO/H₂ oxidation rate ratios on Cs-2.5 in a packed-bed flow reactor. (■) Following standard reduction pretreatment and (◇) following exposure to 1% CO, balance He at 383 K after reduction pretreatment for fresh Cs-2.5 (0.020 g catalyst diluted with 0.5 g acid-washed quartz, 383 K, 1 kPa CO, 1 kPa O₂, 70 kPa H₂, balance He, total flow rate 0.34 cm³ s⁻¹).

The additional role of C* in blocking sites, however, may lead to inaccurate turnover rates when these are normalized by Pt dispersions measured before reaction. The maximum CO oxidation rates (per exposed Pt atom in fresh samples) observed at intermediate Cs surface density (Fig. 4) suggest that some Pt atoms were blocked, but that the residual exposed surfaces were rendered more reactive by inhibited densification of CO monolayers. Alkali atoms are known to increase rates of CO disproportionation to form CO₂ and unreactive C* on Pt [37,50,53,72,73].

The intensity of infrared CO bands after contact with CO at ambient temperature and during catalytic oxidation of H₂-CO mixtures decreases as Cs surface density increases. Linear and bridged CO bands (2100–1900 and 1900–1700 cm⁻¹) decrease with increasing Cs content during contact with 1 kPa CO at 303 K (Fig. 10); similar trends are evident during CO-H₂-O₂ reactions at 383 K (Fig. 11). A new band at ~1340 cm⁻¹, assigned to Cs carbonate, appears on Cs-containing samples during contact with CO at 303 K. Its intensity increases gradually with time (Fig. 12); this band is not detected before reaction, because carbonates formed during exposure to ambient air desorb below H₂ pretreatment temperatures (623 K) [75]. These data indicate that CO₂ forms on Pt/Cs-SiO₂ during contact with CO even at ambient temperatures via CO disproportionation promoted by Cs⁺, as also found on Na-modified Pd/SiO₂ [50]. These reactions form chemisorbed carbon (C*), which irreversibly titrates Pt surface atoms.

Carbonates and C* species form even faster during CO oxidation at 383 K; in fact, C* reached steady-state cov-

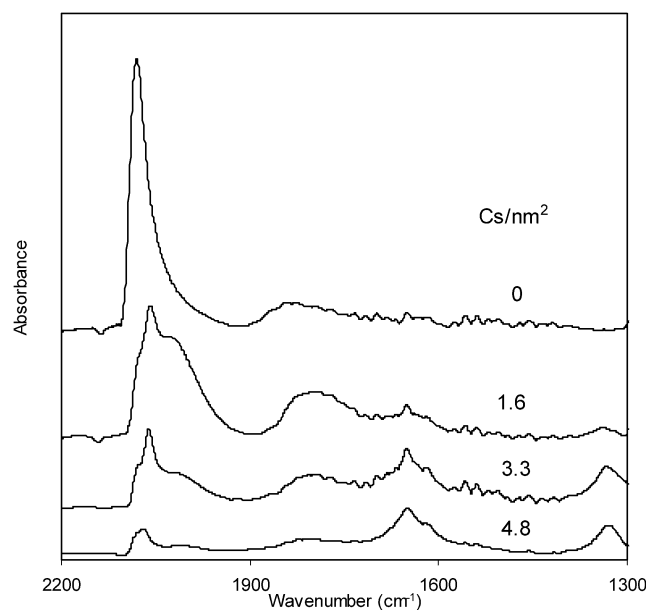


Fig. 10. Infrared spectra of CO adsorbed on promoted and unpromoted 1.6 wt% Pt/SiO₂ catalysts after 3.6 ks exposed to 1% CO, balance He at 303 K, 1 cm³ s⁻¹. The band at 1650 cm⁻¹ is attributed to adsorption of adventitious H₂O by Cs carbonate salts, known to be hygroscopic [74]. Spectra were normalized by the intensity of the Si-O-Si band in the spectra collected in He at 303 K before CO adsorption.

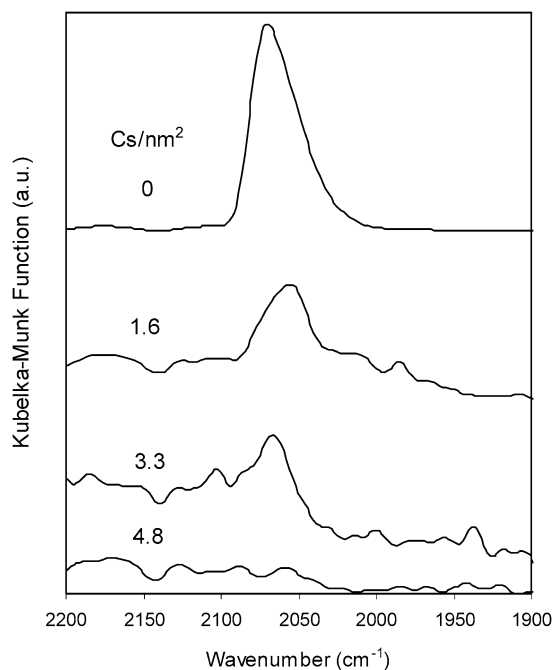


Fig. 11. Infrared spectra of CO adsorbed on promoted and unpromoted 1.6 wt% Pt/SiO₂ catalysts during reaction conditions after 3.6 ks on stream (383 K, 1 kPa CO, 1 kPa O₂, 70 kPa H₂, balance He, total flow rate 0.67 cm³ s⁻¹).

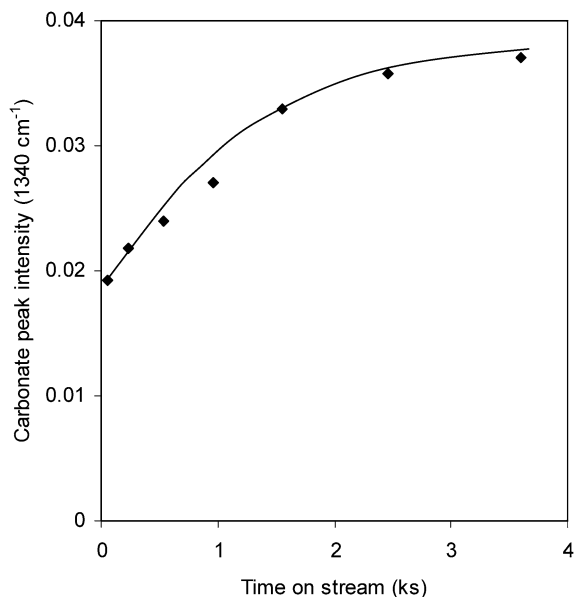


Fig. 12. Intensity of carbonate peak (1340 cm⁻¹) as function of time on stream on the Cs-4.8 sample (1% CO, balance He, 303 K, 1 cm³ s⁻¹). Spectra were normalized by the intensity of the Si–O–Si band in the spectra collected in He at 303 K before CO adsorption.

erages during a few initial CO oxidation turnovers. These conclusions are supported by the complete recovery of initial CO oxidation rates after desorption of adsorbed CO in He at 623 K (Fig. 7). Carbon formation was shown to occur during early stages (<3 ks) of selective CO oxidation reactions on Pt [16], a conclusion confirmed by the data re-

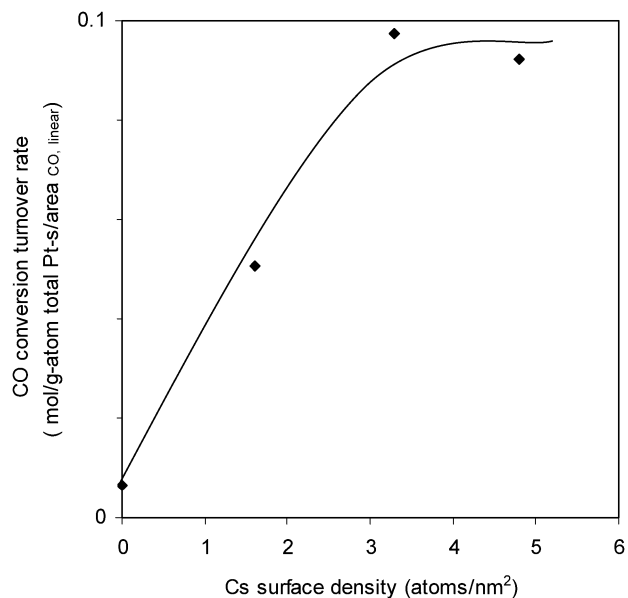


Fig. 13. Effects of Cs surface density on rescaled CO oxidation rate on Pt/SiO₂ during selective CO oxidation. Oxidation rates and selectivities given when the ratio of CO to H₂ oxidation rates reached steady-state value, after ~4.2 ks on stream (0.100 g Pt/SiO₂ and 0.020 g Cs-samples diluted with 0.5 g acid-washed quartz, 383 K, 1 kPa CO, 1 kPa O₂, 70 kPa H₂, balance He, total flow rate 0.67 cm³ s⁻¹). CO oxidation rate rescaled by the total integrated CO area from infrared data taken during in situ reaction after 3.6 ks on stream.

ported here. Since C* formation appears to cease after a few turnovers and the intensity of carbonate bands increases with Cs surface density (Fig. 10), we suggest that Cs promotes CO disproportionation by providing a stoichiometric sink for CO₂ co-products in the form of Cs carbonates.

Turnover rates were rigorously renormalized using the intensity of infrared CO bands as a measure of exposed Pt during reaction. These turnover rates increased monotonically with increasing Cs surface density for all Cs contents (Fig. 13). Thus, Cs increases the reactivity of Pt surface atoms that remain exposed after the formation of chemisorbed C*. The effects of surface blocking and higher reactivity of residual sites combine to give the maximum in turnover rate observed when initial Pt dispersion is nonrigorously used to estimate turnover rates.

The effects of Cs on the reactivity of exposed Pt atoms reflect a role of Cs in the approach of CO oxidation rates to their steady state, which we describe here with the use of first-order “deactivation” dynamics with a rate constant k_d . We note again that such “deactivation” is fully reversed by the desorption of chemisorbed CO in He at 623 K, and thus it does not reflect the initial titration of Pt by unreactive C*, but an increase in the amount of chemisorbed CO (see Section 3.6). During the early stages of reaction, k_d values decreased slightly with increasing Cs content, but k_d values were essentially independent of Cs content at longer times (Fig. 14). We attribute the observed decrease in k_d with Cs content to its promoting effect in the formation of C* species, which inhibit the growth of CO islands on Pt

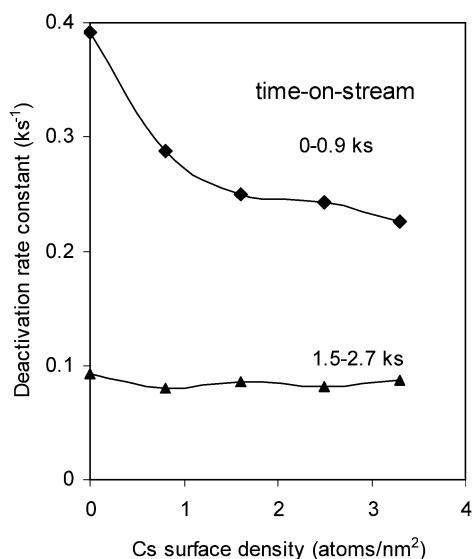


Fig. 14. Deactivation rate constant (k_d) as function of Cs surface density during selective CO oxidation in a packed-bed flow reactor at 383 K (1 kPa CO, 1 kPa O₂, 70 kPa H₂, balance He, total flow rate 0.67 cm³ s⁻¹). k_d was calculated at initial time (◆) and at long time (▲).

surfaces. Chemisorbed carbon can block as many as four CO chemisorption sites [76,77], suggesting that even low C* coverages can markedly disrupt monolayer densification, which occurs over time scales significantly longer than those required for catalytic turnovers (Fig. 8, Section 3.6). Cs-promoted disproportionation decreases k_d by inhibiting CO monolayer growth, a process that causes effective K_1 values to decrease with increasing Cs surface densities. The inverse dependence of r_{CO} on K_1 (Eq. (9)) would then account in a simple manner for the observed monotonic increase in CO oxidation turnover rates as Cs surface density increases (Fig. 13).

Finally, we mention here two other possible effects of alkali on Pt-catalyzed CO oxidation rates. Alkali can influence the structure of Pt clusters, but this appears to be unlikely in light of the weak effects of alkali on Pt dispersion (Table 1) compared with the strong effects of alkali on CO oxidation turnover rates (Fig. 4). Moreover, CO and H₂ oxidation reactions are widely regarded as structure-insensitive and thus would be weakly influenced by any alkali-induced structural changes [78,79].

Electronic interactions between alkali atoms and metals are often invoked to account for the catalytic effects of alkali on metal-catalyzed reactions [36,53,80–82]. Electrochemical [83], chemisorption [84–87], and theoretical [88] studies indicate that alkali weakens C–O and O–O π bonds in adsorbed CO and O₂ while strengthening M–C and M–O bonds, which benefit from higher electron density at alkali-promoted metal (M) surfaces. These electronic effects do not influence H–H σ -bonds in H₂. As a result, electropositive atoms increase CO and O₂ dissociation rates on metals [83,88]. CO dissociation steps are not required for CO oxidation, but they are involved in disproportionation reactions

Table 4

Effect of promoter identity on CO oxidation rates and selectivities (383 K, 1 kPa CO, 1 kPa O₂, 70 kPa H₂, balance He, total flow 0.67 cm³ s⁻¹). Oxidation rates (r_{CO}) and selectivities (S_{CO}) given when the ratio of CO to H₂ oxidation rates reached steady-state value, after ~4.2 ks on stream. Surface silanols were measured by infrared spectroscopy at 323 K in He flow after treatment in He at 623 K for 0.9 ks

Sample	r_{CO} (10 ⁻² mol/(g-atom-surface-Pt s))	S_{CO} (%)	Fraction of silanol titrated (%)	Polarizability (monovalent cation) ^a
Pt/SiO ₂	5.1	63	0	–
Na-1.6	3.7	95	67	0.03
Rb-1.6	26.6	95	76	1.90
Cs-1.6	30.0	90	80	2.90

^a Ref. [81].

that form unreactive C*. O₂ dissociation is promoted to a greater extent than CO dissociation [83], and this elementary step is involved and kinetically relevant in the oxidation of CO and H₂; its corresponding rate constant (k_3) appears in both rate equations (Eqs. (9) and (10)). Thus, the observed effects of Cs on CO oxidation rates may also reflect, at least in part, a higher k_3 value arising from electronic effects of Cs cations on Pt surfaces. Such effects would influence CO and H₂ oxidation rates to the same extent; thus, R (Eq. (8)) would not be influenced by these electronic effects; indeed, alkali identity influences R only weakly (Table 4). A clear deconvolution of electronic effects from the other processes discussed here is not possible, because of the concurrent effects of alkali on R via inhibition of spillover-mediated H₂ oxidation pathways. In effect, oxidation rates depend on the product of k_3 and the density of free sites, and the respective effects of alkali on each cannot be decoupled from steady-state rate measurements.

3.8. Effect of alkali identity on CO oxidation turnover rates and selectivities

Table 4 shows CO oxidation rates (based on initial Pt dispersion) and CO oxidation selectivities on 1.6 wt% Pt/SiO₂ modified with Na, Rb, or Cs (1.6 atoms/nm²). All three samples gave CO oxidation selectivities above 90%, apparently because all alkali atoms stoichiometrically titrate silanols and thus inhibit spillover-mediated H₂ oxidation pathways. CO oxidation turnover rates on Pt/SiO₂ and Na-1.6 were similar and much lower than those measured on samples modified by Rb or Cs. More polarizable cations tend to promote CO and O₂ dissociation more effectively [36,37,88] and lead to higher CO oxidation rates. These stronger effects of Cs and Rb are consistent with the lower vibrational frequencies for CO adsorbed on samples modified or promoted with Cs and Rb than on those modified by Na (Fig. 15), which shows that C–O bonds become weaker with increasing cation polarizability [37,50,53,72,73]. These results also suggest that Rb and Cs function similarly in their ability to modify Pt sites and increase CO oxidation rates and selectivities in H₂-rich streams.

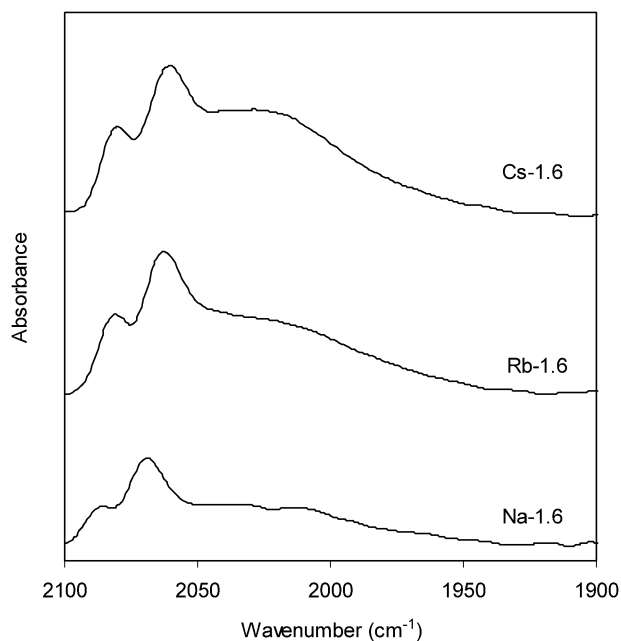


Fig. 15. Infrared spectra of CO adsorbed on alkali-modified samples after 3.6 ks exposed to 1% CO, balance He at 303 K, $1 \text{ cm}^3 \text{ s}^{-1}$. Spectra were normalized by the intensity of the Si–O–Si band in the spectra collected in He at 303 K before CO adsorption.

We note here that these materials merit further study with realistic streams containing significant concentrations of H_2O and CO_2 , which may interact with alkali promoters and influence the effect of alkali on rates and stability.

4. Conclusions

Pt clusters dispersed on Cs-modified SiO_2 are active and selective catalysts for CO oxidation in H_2 -rich streams. Infrared spectra showed that alkali ions titrate Si–OH groups in silica and inhibit spillover-mediated H_2 oxidation pathways that decrease CO oxidation selectivities; these spillover-mediated pathways are unaffected by competitive adsorption of CO and lead to significant selectivity losses during preferential oxidation of CO in H_2 -containing streams. Alkali also increased monofunctional CO oxidation turnover rates on Pt surfaces, apparently by disrupting densification of adsorbed CO monolayers via unreactive C^* formed via dissociation or disproportionation of CO. Such densification processes are evident from the gradual decrease in CO oxidation rates and the concurrent increase in the intensity of infrared bands for chemisorbed CO observed during initial stages of contact with H_2 –CO– O_2 reactant mixtures. These conclusions are consistent with the recovery of initial rates by desorption of adsorbed CO in He at high temperatures and with the observed increase in CO oxidation selectivity with time on stream. Alkali cations (Na, Rb, Cs) titrate Si–OH groups stoichiometrically and lead to similar promotion of CO oxidation selectivity by suppressing spillover-mediated H_2 oxidation. Electropositive cations, such as Rb and Cs, increased

rates of CO oxidation on Pt clusters more effectively than Na cations. Modification of SiO_2 with 1.6 Cs nm^{-2} led to Pt clusters with much higher CO oxidation turnover rates relative to those on Pt/ SiO_2 samples with similar Pt dispersion. CO oxidation selectivities greater than 90% are characteristic of Pt clusters, even at H_2/CO ratios of ~ 100 ; lower selectivities reported previously reflect significant contributions from spillover-mediated H_2 oxidation pathways on support surfaces.

Acknowledgments

This study was supported in part by Nippon Steel Corporation through an unrestricted grant to the Laboratory for the Science and Applications of Catalysis and to the Berkeley Catalysis Center. C.P. acknowledges a postdoctoral fellowship from the Ministerio de Educacion, Cultura y Deporte (Spain). T.W. acknowledges the financial support of the Japan Cooperation Center, Petroleum, and Nippon Oil Co. for his research stay at the University of California at Berkeley. E.I. acknowledges technical discussions with Drs. Daniel Loffler and Tae-Yun Park.

References

- [1] R. Farrauto, S. Hwang, L. Shore, W. Ruettinger, J. Lampert, T. Giroux, Y. Liu, O. Ilinich, *Annu. Rev. Mater. Res.* 33 (2003) 1.
- [2] A. Manasilp, E. Gulari, *Appl. Catal. B* 225 (2004) 489.
- [3] S.H. Oh, R.M. Sinkevitch, *J. Catal.* 142 (1993) 254.
- [4] A. Sirijaruphan, J.G. Goodwin Jr., R.W. Rice, *J. Catal.* 221 (2004) 288.
- [5] H. Igarashi, H. Uchida, M. Suzuki, Y. Sasaki, M. Watanabe, *Appl. Catal. A* 159 (1997) 159.
- [6] M.J. Kahlich, H.A. Gasteiger, R.J. Behm, *J. Catal.* 171 (1997) 93.
- [7] M.M. Schubert, V. Plzak, J. Garcke, R.J. Behm, *Catal. Today* 76 (2001) 143.
- [8] B. Schumacher, Y. Denkwitz, V. Plzak, M. Kinne, R.J. Behm, *J. Catal.* 224 (2004) 449.
- [9] R.M. Torres Sanchez, A. Ueda, K. Tanaka, M. Haruta, *J. Catal.* 168 (1997) 125.
- [10] Y. Tanaka, T. Utaka, R. Kikuchi, K. Sasaki, K. Eguchi, *Appl. Catal. A* 238 (2003) 11.
- [11] Y.F. Han, M.J. Kahlich, M. Kinne, R.J. Behm, *Phys. Chem. Chem. Phys.* 4 (2002) 389.
- [12] S. Ito, T. Fujimori, K. Nagashima, K. Yuzaki, K. Kunimori, *Catal. Today* 57 (2000) 247.
- [13] J.L. Margitfalvi, M. Hegedus, A. Szegedi, I. Sajo, *Appl. Catal. A* 272 (2004) 87.
- [14] G.B. Bethke, H.H. Kung, *Appl. Catal. A* 194–195 (2000) 43.
- [15] O. Korotkikh, R. Farrauto, *Catal. Today* 62 (2000) 249.
- [16] A. Sirijaruphan, J.G. Goodwin Jr., R.W. Rice, *J. Catal.* 224 (2004) 304.
- [17] M.M. Schubert, M.J. Kahlich, G. Feldmeyer, M. Huttner, S. Hackenberg, H.A. Gasteiger, R.J. Behm, *Phys. Chem. Chem. Phys.* 3 (2001) 1123.
- [18] I.H. Son, A.M. Lane, *Catal. Lett.* 76 (2001) 151.
- [19] M. Watanabe, H. Uchida, K. Ohkubo, H. Igarashi, *Appl. Catal. B* 46 (2003) 595.
- [20] H. Tanaka, S. Ito, S. Kameoka, K. Tomishige, K. Kunimori, *Appl. Catal. A* 250 (2003) 255.
- [21] S. Ito, H. Tanaka, Y. Minemura, S. Kameoka, K. Tomishige, K. Kunimori, *Appl. Catal. A* 273 (2004) 295.

- [22] J.H. Sinfelt, P.J. Lucchesi, *J. Am. Chem. Soc.* 85 (1963) 3365.
- [23] M.A. Vannice, C.C. Twu, *J. Catal.* 82 (1983) 213.
- [24] M.A. Vannice, C. Sudhakar, *J. Phys. Chem.* 88 (1984) 2429.
- [25] B. Sen, M.A. Vannice, *J. Catal.* 113 (1988) 52.
- [26] M.A. Vannice, B. Sen, *J. Catal.* 115 (1989) 65.
- [27] E.V. Benvenuto, L. Franken, C.C. Moro, C.U. Davanzo, *Langmuir* 15 (1999) 8140.
- [28] M. Lacroix, G.M. Pajonk, S.T. Teichner, *J. Catal.* 101 (1986) 314.
- [29] J.T. Miller, B.L. Meyers, F.S. Modica, G.S. Lane, M. Vaarkamp, D.C. Koningsberger, *J. Catal.* 143 (1993) 395.
- [30] G.B. McVicker, M.A. Vannice, *J. Catal.* 63 (1980) 25.
- [31] J. Wei, E. Iglesia, *J. Phys. Chem. B* 108 (2004) 4094.
- [32] J.E. Benson, M. Boudart, *J. Catal.* 4 (1965) 704.
- [33] E. Iglesia, J.E. Baumgartner, G.L. Price, K.D. Rose, J.L. Robbins, *J. Catal.* 125 (1990) 95.
- [34] J.A. Biscardi, G.D. Meitzner, E. Iglesia, *J. Catal.* 179 (1998) 192.
- [35] P. Kubelka, F.Z. Munk, *Technol. Phys.* 12 (1931) 593.
- [36] M. Konsolakis, I.V. Yentekakis, *Appl. Catal. B* 29 (2001) 103.
- [37] J.S. Rieck, A.T. Bell, *J. Catal.* 100 (1986) 305.
- [38] M. McLaughlin, M.M. McClory, R.D. Gonzalez, *J. Catal.* 89 (1984) 392.
- [39] K. Aika, K. Shimakazi, Y. Hattori, A. Ohya, S. Ohshima, K. Shirota, A. Ozaki, *J. Catal.* 92 (1985) 296.
- [40] J. Korah, W.A. Spieker, J.R. Regalbuto, *Catal. Lett.* 85 (2003) 123.
- [41] M. Schreier, J.R. Regalbuto, *J. Catal.* 225 (2004) 190.
- [42] W.A. Spieker, J.R. Regalbuto, *Stud. Surf. Sci. Catal.* 130 (2000) 203.
- [43] K.Ch. Akrapotulu, L. Vordonis, A. Lycourghiotis, *J. Catal.* 109 (1988) 41.
- [44] M.M. Schubert, M.J. Kahlich, H.A. Gasteiger, R.J. Behm, *J. Power Sources* 84 (1999) 175.
- [45] J.L. Gland, B.A. Sexton, G.B. Fisher, *Surf. Sci.* 95 (1980) 587.
- [46] D.O. Uner, M. Pruski, T.S. King, *Top. Catal.* 2 (1995) 59.
- [47] D.O. Uner, M. Pruski, T.S. King, *J. Catal.* 156 (1995) 60.
- [48] G.M. Pajonk, *Appl. Catal. A* 202 (2000) 157.
- [49] E.F. Vansant, P. Van Der Voort, K.C. Vrancken, *Stud. Surf. Sci. Catal.* 93 (1995) 65.
- [50] L.F. Liotta, G.A. Martin, G. Deganello, *J. Catal.* 164 (1994) 322.
- [51] V. Pitchon, M. Primet, H. Praliaud, *Appl. Catal.* 62 (1990) 317.
- [52] M.J. Kappers, J.T. Miller, D.C. Koningsberger, *J. Phys. Chem.* 100 (1996) 3227.
- [53] T. Okuhara, H. Tamura, M. Misono, *J. Catal.* 95 (1985) 41.
- [54] P.A.J.M. Angevaere, H.A.C.M. Hendrickx, V. Ponc, *J. Catal.* 110 (1988) 11.
- [55] N.W. Cant, D.E. Angove, *J. Catal.* 97 (1986) 36.
- [56] N.W. Cant, R.A. Donaldson, *J. Catal.* 71 (1981) 320.
- [57] D.M. Haaland, F.L. Williams, *J. Catal.* 76 (1982) 450.
- [58] P.T. Fanson, W.N. Delgass, J. Lauterbach, *J. Catal.* 204 (2001) 35.
- [59] R.A. Herderson, J.T. Yates, *Surf. Sci.* 268 (1992) 189.
- [60] R.J. Behm, P.A. Thiel, P.R. Norton, P.E. Bindner, *Surf. Sci.* 147 (1984) 143.
- [61] J. Lauterbach, H.H. Rotermund, *Surf. Sci.* 311 (1994) 231.
- [62] J. Sarkany, M. Bartok, R.D. Gonzalez, *J. Catal.* 81 (1983) 347.
- [63] V.V. Gorodetskii, W. Drachsel, *Appl. Catal. A* 188 (1999) 267.
- [64] R.A. Shigeishi, D.A. King, *Surf. Sci.* 75 (1978) L397.
- [65] S. Ladas, R. Imbihl, G. Ertl, *Surf. Sci.* 198 (1988) 42.
- [66] M.A. Barteau, E.I. Ko, R.J. Madix, *Surf. Sci.* 104 (1981) 4161.
- [67] A. Crossley, D.A. King, *Surf. Sci.* 95 (1980) 131.
- [68] E.D. Williams, P.A. Thiel, W.H. Weinberg, J.T. Yates, *J. Chem. Phys.* 72 (1980) 3496.
- [69] J.M. White, *J. Phys. Chem.* 87 (1983) 915.
- [70] J.L. Gland, E.B. Kollin, *J. Phys. Chem.* 78 (1983) 963.
- [71] B.E. Nieuwenhuys, *Surf. Sci.* 126 (1983) 307.
- [72] K.M. Bailey, T.K. Campbell, J.L. Falconer, *Appl. Catal.* 54 (1989) 159.
- [73] C.T. Campbell, D.W. Goodman, *Surf. Sci.* 123 (1982) 413.
- [74] J.R. Monnier, J.L. Stavinoha, R.L. Minga, *J. Catal.* 226 (2004) 401.
- [75] E.J. Duskocil, R.J. Davis, *J. Catal.* 188 (1999) 353.
- [76] V. Mantolin, E. Gillet, *Surf. Sci.* 238 (1990) 75.
- [77] I. Stara, V. Mantolin, *Surf. Sci.* 313 (1994) 99.
- [78] M. Boudart, F. Rumpf, *React. Kinet. Catal. Lett.* 35 (1987) 95.
- [79] F.V. Hanson, M. Boudart, *J. Catal.* 53 (1978) 56.
- [80] J.R. Monnier, G.W. Hartley, *J. Catal.* 203 (2001) 253.
- [81] R.B. Grant, R.M. Lambert, *J. Catal.* 93 (1985) 92.
- [82] S.A. Tan, R.B. Grant, R.M. Lambert, *J. Catal.* 106 (1987) 54.
- [83] I.V. Yentekakis, G. Moggridge, C.G. Vayenas, R.M. Lambert, *J. Catal.* 146 (1994) 292.
- [84] J.C. Bertolini, P. Delichere, J. Massardier, *Surf. Sci.* 160 (1985) 531.
- [85] I.R. Harkness, R.M. Lambert, *J. Chem. Soc. Faraday Trans.* 93 (1997) 1425.
- [86] E.L. Garfunkel, J.E. Crowell, G.A. Somorjai, *J. Phys. Chem.* 86 (1982) 310.
- [87] E.L. Garfunkel, J.E. Crowell, G.A. Somorjai, *Surf. Sci.* 121 (1982) 303.
- [88] N.D. Lang, S. Holloway, J.K. Norskov, *Surf. Sci.* 150 (1985) 24–38.